

Magnetic excitations in SrCu₂O₃: a Raman scattering study

A. Göbbling, U. Kuhlmann, and C. Thomsen

Institut für Festkörperphysik, Technische Universität Berlin, Hardenbergstr. 36, D-10623 Berlin, Germany

A. Löffert, C. Gross, and W. Assmus

Physikalisches Institut, J.W. Goethe-Universität, Robert-Mayer-Str. 2-4, D-60054 Frankfurt a. M., Germany

(Dated: 6 February 2003)

We investigated temperature dependent Raman spectra of the one-dimensional spin-ladder compound SrCu₂O₃. At low temperatures a two-magnon peak is identified at $3160 \pm 10 \text{ cm}^{-1}$ and its temperature dependence analyzed in terms of a thermal expansion model. We find that the two-magnon peak position must include a cyclic ring exchange of $J_{cycl}/J_{\perp} = 0.09 - 0.25$ with a coupling constant along the rungs of $J_{\perp} \approx 1215 \text{ cm}^{-1}$ (1750 K) in order to be consistent with other experiments and theoretical results.

PACS numbers: 78.30.-j, 75.50.Ee

Antiferromagnetic copper oxide spin-ladders have been investigated intensively from a theoretical and experimental point of view.¹ Superconducting under high pressure² they form a bridge between 1D Heisenberg chains and a 2D Heisenberg square-lattice, which is also a model for high- T_C superconductors. The magnetic ground state of a spin ladder is surprisingly not a long ranged Néel state but a short ranged resonating valence bond state.³ The first excited state is separated from the ground state by a finite energy Δ . The spin gap was first predicted theoretically^{4,5} and later confirmed experimentally.⁶

Typical realizations of a two-leg spin-ladder are the compounds SrCu₂O₃ (Ref. 7) and (Sr,Ca,La)₁₄Cu₂₄O₄₁.⁸ The first compound is a prototype of weakly coupled Cu₂O₃ spin-ladders while the latter consists of a ladder and a Cu₂O edge sharing chain part. In contrast to SrCu₂O₃, (Sr,Ca,La)₁₄Cu₂₄O₄₁ is intrinsically doped with holes. A schematic view of the compound SrCu₂O₃ is shown in Fig. 1. Cu atoms, represented by d -orbitals, are antiferromagnetically coupled via an intermediate oxygen p -orbital by superexchange⁹. The Sr atoms are located in between the planes containing the Cu₂O₃ atoms. The coupling constants along the legs and the rungs are denoted with J_{\parallel} and J_{\perp} . The interladder coupling is negligible to first approximation because the superexchange via a Cu-O-Cu path with a 90° bond angle has a smaller orbital overlap than with a bond angle of 180°.¹⁰ Thus, a ladder can be considered an isolated quasi one-dimensional object with a Heisenberg Hamiltonian $H = J_{\perp} \sum_{\text{rung}} \mathbf{S}_i \cdot \mathbf{S}_j + J_{\parallel} \sum_{\text{leg}} \mathbf{S}_i \cdot \mathbf{S}_j$. In the literature coupling ratios $J_{\parallel}/J_{\perp} \sim 1.7 - 2.0$ have been reported^{11,12} taking the Hamiltonian mentioned above into account for analyzing the data. On the other hand with almost identical Cu-Cu distances in leg and rung direction^{7,8,13} one would expect an isotropic ratio $J_{\parallel}/J_{\perp} \sim 1$. This picture was also confirmed by an analysis of optical conductivity data.¹⁴ Recently the inclusion of a cyclic ring exchange J_{cycl} was suggested in order to resolve the discrepancy between the geo-

metrical considerations and $J_{\parallel}/J_{\perp} \sim 1.7 - 2.0$.^{15,16,17} This ring exchange can be understood as a superposition of clockwise and counter clockwise permutations of four spins around a plaquette (positions ABCD in Fig. 1). A term $H_{cycl} = J_{cycl} \sum_i K_{ABCD}^i$ with $K_{ABCD} = (\mathbf{S}_A \mathbf{S}_B)(\mathbf{S}_C \mathbf{S}_D) + (\mathbf{S}_A \mathbf{S}_D)(\mathbf{S}_B \mathbf{S}_C) - (\mathbf{S}_A \mathbf{S}_C)(\mathbf{S}_B \mathbf{S}_D)$ has to be added to the conventional Heisenberg Hamiltonian H .¹⁸ In order to achieve the isotropic limit of $J_{\parallel}/J_{\perp} \sim 1$ a ring exchange of $J_{cycl}/J_{\perp} \sim 0.18 - 0.30$ was introduced.^{16,17}

In this paper we studied the Raman spectra of the two leg $S = \frac{1}{2}$ spin-ladder compound SrCu₂O₃. In addition to phonons we investigated the two-magnon peak in this compound at temperatures between 25 K and 300 K. We find that the inclusion of a ring exchange is necessary for the understanding of the magnetic properties of SrCu₂O₃.

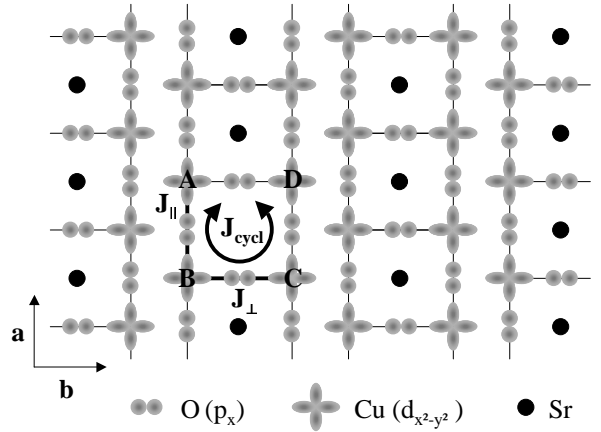


FIG. 1: Schematic view of the two-leg ladder SrCu₂O₃ projected on the ab -plane. The Sr atoms are located in between the planes containing the Cu₂O₃ atoms. The magnetic coupling constants along the rungs and the legs are indicated by J_{\perp} and J_{\parallel} and the cyclic ring exchange by J_{cycl} . The coupling between two Cu d -orbitals is caused by superexchange interaction via an O p -orbital.

Polycrystalline SrCu_2O_3 was grown under high pressure as described by Löffert *et al.*¹⁹ The crystallographic structure was verified by x-ray diffraction. In addition to SrCu_2O_3 small amounts of $\text{Sr}_2\text{Cu}_3\text{O}_5$, CuO and Cu_2O were detected. Measurements were performed using a LabRam spectrometer (Dilor) including a grating with 600 and 1800 grooves/mm in backscattering geometry and a multichannel CCD detector. An Ar^+ laser spot (488 nm) was focused by a $80 \times$ microscope objective on small individual crystallites on the sample surface with a diameter of 1-2 μm . The spectra in Fig. 2 were measured at room temperature. The crystallite was chosen by using a polarization microscope:²⁰ The sample surface was illuminated normally with linear polarized white light. The reflected light was detected through an analyzer crossed to the polarizer with a CCD camera. Being an anisotropic material the reflected light is in general elliptically polarized. As for the ladder compound $\text{LaCuO}_{2.5}$,²⁰ we assume the direction along the ladder (a -axis) to be the one with the largest anisotropy in SrCu_2O_3 , whereas the b and c axes are approximately optically isotropic. Thus, there should be a difference in brightness along and perpendicular to the a -axis when rotating the sample. If the incident wave vector \mathbf{k}_i is parallel to the a -axis the image stays dark while rotating the sample. For $\mathbf{k}_i \perp a$ the crystallite appears dark and bright for four times when turning the sample 360° . The spectra in Fig. 2 were measured on a crystallite for $\mathbf{k}_i \perp a$. For our measurements down to 25 K (spectra in Fig. 3) the sample was mounted on the cold finger of an Oxford microcryostat.

The Raman spectra of SrCu_2O_3 can be divided into a low (100-1700 cm^{-1}) and a high-energy (2000-4600 cm^{-1}) region as shown in Figs. 2 and 3. We verified the chemical composition of our polycrystalline sample by an analysis of the phonons in the low energy part of the spectra. We start with a factor group analysis (FGA) of the vibrational modes according to Rousseau *et al.*²¹ The unit cell of SrCu_2O_3 consists of two formula units. Structure analysis^{7,22} attributes SrCu_2O_3 to the space group $Cmmm$ (D_{2h}^{19}). The FGA results in

$$\Gamma_{\text{SrCu}_2\text{O}_3} = 2A_g + 4B_{1u} + 2B_{1g} + 4B_{2u} + 4B_{3u} + 2B_{3g} \quad (1)$$

Having a center of inversion only even modes show Raman activity, resulting in six Raman active phonons. We expect the two A_g modes in the spectra measured in parallel polarization while the four even B modes should be observed in crossed polarization.

Figure 2 shows four spectra measured at $T=295$ K two in parallel and two in crossed polarization. The axes were identified using the described analysis with polarized light; comparing Fig. 2 to the spectra of the very similar ladder compound $\text{Sr}_{14}\text{Cu}_{24}\text{O}_{41}$,^{12,23,24,25} we identify the a (leg) and b (rung) axes as indicated in the figure.²⁶

In (bb) polarization only a single phonon at 550 cm^{-1} is observed, while in (aa) two phonons at 310, 550 cm^{-1} , and in addition several broad peaks around 1150 cm^{-1} are visible. We assign these two phonons as the two al-

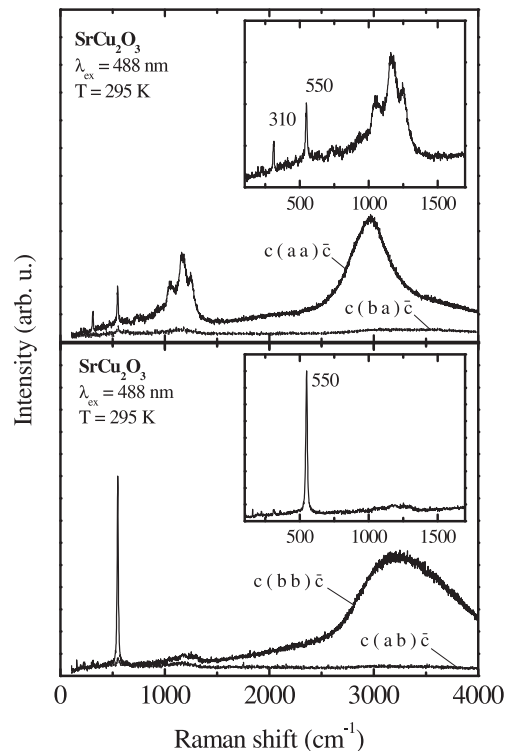


FIG. 2: Raman spectra in parallel and crossed polarization measured at $T=295$ K. The insets show the low energy parts of the spectra measured in parallel polarization.

lowed A_g modes. In $\text{Sr}_{14}\text{Cu}_{24}\text{O}_{41}$ modes at 316 cm^{-1} and 549 cm^{-1} were observed.²³ The latter is believed to be the breathing mode of the O-ladder atoms located on the ladder legs²³, which is in accordance with our assignment. The structure at about 1150 cm^{-1} was also observed in $\text{Sr}_{14}\text{Cu}_{24}\text{O}_{41}$, its origin attributed to two-phonon processes.^{23,27} Knowing only few phonons at the Γ point the details of the broad structure around 1150 cm^{-1} in SrCu_2O_3 remain unclear. In summary, we identified the two allowed A_g ladder phonons at 310 and 550 cm^{-1} in SrCu_2O_3 at room temperature, the B_{1g} modes were too weak to be observed, and the B_{3g} not allowed for our geometry.

In Fig. 2 in addition to the phonons a peak around 3000 cm^{-1} was observed in (aa) and (bb) polarizations while it was absent in the crossed polarizations (ab) and (ba) . It can be shown from the two-magnon Raman Hamiltonian²⁸ that for a two-leg Heisenberg ladder the two-magnon peak is forbidden in all crossed polarizations. The observed spectra follow the selection rules of a two-magnon peak.

In Fig. 3 the Raman spectra of the high-energy region are presented for different temperatures. The spectra were measured on another crystallite between 25 K and 300 K. Comparing them to the aligned spectra in Fig. 2 we assign the upper spectrum as (aa) and the lower one as (bb) polarized. In (aa) polarization a sharp peak is visible which broadens and shifts to lower energies

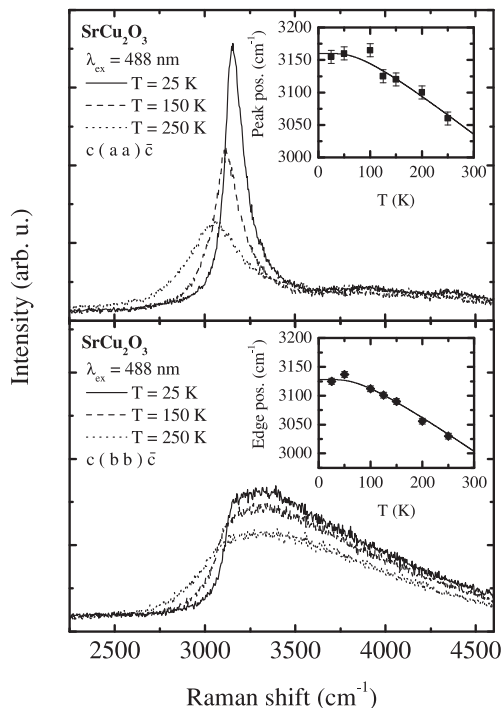


FIG. 3: Raman spectra measured with the same polarization as in Fig. 2 with $\lambda_{ex} = 488$ nm at 25 K (solid), 150 K (dashed) and 250 K (dotted). Insets: peak positions (top) and edge position (bottom) of the two-magnon peak as a function of temperature.

with increasing temperature. In (bb) polarization a much broader peak is measured; it remains broad also down to the lowest temperatures. We identify these features to be the two-magnon peaks which were also observed in $\text{Sr}_{14}\text{Cu}_{24}\text{O}_{41}$ at a lower energy (maximum for $T=8-20$ K at $2900-3000$ cm^{-1}).^{12,23,24,25} The energy of the peak maxima as a function of temperature is shown in the upper inset of Fig. 3. In (bb) polarization the left edge position is plotted as a function of temperature in the lower insets of Fig. 3 due to difficulties in determining the precise peak maxima. The two-magnon peak shifts for $T > 75$ K almost linearly with temperature and saturates at low temperatures at 3160 cm^{-1} (peak position) and 3130 cm^{-1} (edge position).

Using a simple model of thermal expansion we are able to understand the temperature dependence of these peaks. The starting point is a system containing two copper d -orbitals and one intermediate oxygen p -orbital with a 180° bond angle as found in flat ladder compounds, hence the model is not only applicable to SrCu_2O_3 but also, e.g., to $\text{Sr}_{14}\text{Cu}_{24}\text{O}_{41}$. The two copper atoms are coupled by superexchange with the coupling constant J . We assume that the two-magnon energy scales linearly with J . The average distance d between two copper atoms is a function of temperature. Due to an anharmonic interatomic potential the average distance increases in first order as $d = d_0 + A\omega/(\exp(\omega/T) - 1)$, where d_0 is the distance at $T=0$ K, A is a constant, rep-

resenting the strength of the expansion, and ω is an averaged phonon energy (Einstein model). Within the three-band Hubbard-model J equals $4t_{pd}^4/\varepsilon_{pd}^2(Ud^{-1} + \varepsilon_{pd}^{-1})$ with t_{pd} being the overlap integral between Cu-O sites, U the Coulomb repulsion, and ε_{pd} the charge transfer energy.²⁹ The overlap integral $t_{pd} \propto d^{-4}$ and the Coulomb repulsion $U \propto d^{-1}$ are a functions of d as shown by Harrison.³¹ (p. 643) Using the parameters $C_{1,2}$, J can be written as

$$J = C_1 d^{-15} + C_2 d^{-16} \quad (2)$$

The temperature dependence of the two-magnon energy, which is proportional to J , arises from a Taylor expansion around d_0 .

$$E_{2-mag} = E_0 - \frac{B\omega}{\exp(\omega/T) - 1} \quad (3)$$

E_0 is the two-magnon energy at $T=0$ K, B is a dimensionless constant proportional to A , and ω is the averaged phonon frequency. Other power-law exponents in Eq. 2 have been used in similar systems in the literature (e.g., Kawada *et al.*³⁰); the further analysis does not depend much on this choice as long B is simply a parameter. The temperature dependence of the peak/edge maxima of both spectra in the insets of Fig. 3 were fitted simultaneously using Eq. (3) with the parameters $B = 0.94 \pm 0.05$, $\omega = 160 \pm 10$ cm^{-1} , $E_0(aa) = 3160 \pm 10$ cm^{-1} and $E_0(bb) = 3130 \pm 10$ cm^{-1} . The fit shows excellent agreement with the experimental data. The averaged phonon frequency ω is comparable to those of high- T_C cuprate materials.³² The different values for E_0 in the (aa) and (bb) spectra in Fig. 3 are caused by the difference between peak edge and peak maximum. For the further analysis we take only the energy $E_0(aa)=3160$ cm^{-1} into account. The observed temperature dependence is in accordance with the assumed magnetic origin of the peak. The common picture of superexchange is confirmed by our measurements.

We now show that in order to compare the energy E_0 with existing experiments and theoretical results in a consistent way the cyclic ring exchange must be included. Note, that it is not possible to determine the magnetic constants and the spin gap directly from the two-magnon peak position. In order to obtain these values from our spectra we have to make several assumptions based on calculations: (i) *Ab initio* calculations¹⁰ yielded $J_{\parallel}/J_{\perp} = 1.1$ for the coupling constant ratio. This ratio is also close to the isotropic limit, which can be deduced from geometrical considerations. (ii) We include a ring exchange of $J_{cycl}/J_{\perp} = 0.09 - 0.25$. Cyclic ring exchange values on the same order ($J_{cycl}/J_{\perp} = 0.18 - 0.30$) have also been introduced for the comparable two-leg spin ladder compound $(\text{La,Ca})_{14}\text{Cu}_{24}\text{O}_{41}$ (Refs. 16,17). (iii) Schmidt *et al.* have shown recently in a theoretical Raman study for a Heisenberg two-leg ladder with $J_{\parallel}/J_{\perp} = 1.2$ and $J_{cycl}/J_{\perp} = 0.2$ that the two-magnon peak maximum should be located at $E_0 \approx 2.6 \cdot J_{\perp}$.¹⁸ Because the ratio $J_{\parallel}/J_{\perp} = 1.2$ is slightly larger than the

one stated above for SrCu_2O_3 we take $E_0/J_\perp = 2.6 \pm 0.1$ for a further analysis. (iv) Calculating the spin gap we use the expression $\Delta \approx 0.48 \cdot J_\perp - 1.08 \cdot J_{\text{cycl}}$ which has been derived by Nunner *et al.*¹⁷ for a two-leg Heisenberg ladder with ring exchange having adjusted for the different definitions of J_{cycl} . The expression for Δ is valid approximately in the range $J_\parallel/J_\perp = 1.0 - 1.3$. As a result we obtain from our experiment $J_\perp = 1170 - 1260 \text{ cm}^{-1}$ (1680 - 1810 K) for the coupling constant. Taking $J_\perp = 1215 \text{ cm}^{-1}$ results in $\Delta = 260 - 470 \text{ cm}^{-1}$ (380 - 680 K) for the spin gap. The latter value is in good agreement with spin gap values measured with susceptibility (420 K),⁶ NMR (680 K)^{6,33,34} and neutron scattering (380 K) on $\text{Sr}_{14}\text{Cu}_{24}\text{O}_{41}$.¹¹ In contrast, excluding the spin exchange coupling would yield a spin gap value of approximately 840 K, which is out of scale by a factor of 1.2 - 2.2 when comparing to the experiments mentioned. Our experiment thus supports the presence of a four spin ring exchange on the order of $J_{\text{cycl}}/J_\perp = 0.09 - 0.25$. The lower limit of J_{cycl}/J_\perp so obtained corresponds to Δ from

NMR, the upper one to Δ from neutron scattering.

In conclusion we found the two allowed A_g phonons at 310 cm^{-1} and 550 cm^{-1} in SrCu_2O_3 and studied the magnetic excitations in this compound. A peak with an energy of $3160 \pm 10 \text{ cm}^{-1}$ at low temperatures starts to shift to lower energies with increasing temperature. We identified this peak as the two-magnon peak and confirmed this by its temperature dependence. We derived a simple expression which describes excellently the peak energy as a function of temperature. For low temperatures we are able to explain the two-magnon peak energy $E_0 = 3160 \text{ cm}^{-1}$ in accordance with existing theoretical and experimental results by including a cyclic ring exchange using the values: $J_\parallel/J_\perp = 1.1$, $J_{\text{cycl}}/J_\perp = 0.09 - 0.25$, $J_\perp \approx 1215 \text{ cm}^{-1}$ (1750 K) and $\Delta = 260 - 470 \text{ cm}^{-1}$ (380 - 680 K).

We thank K. P. Schmidt and G. S. Uhrig for helpful and valuable discussions. This work was supported by the Deutsche Forschungsgemeinschaft, SPP 1073.

-
- ¹ E. Dagotto and T. M. Rice, *Science* **271**, 618 (1996).
² M. Uehara, T. Nagata, J. Akimitsu, H. Takahashi, N. Mōri, and K. Kinoshita, *J. Phys. Soc. J.* **65**, 2764 (1996).
³ P. W. Anderson, *Nature* **235**, 1196 (1987).
⁴ E. Dagotto, J. Riera, and D. Scalapino, *Phys. Rev. B* **45**, 5744 (1992).
⁵ T. M. Rice, S. Gopalan, and M. Sigrist, *Europhys. Lett.* **23**, 445 (1993).
⁶ M. Azuma, Z. Hiroi, M. Takano, K. Ishida, and Y. Kitaoka, *Phys. Rev. Lett.* **73**, 3463 (1994).
⁷ Z. Hiroi, M. Azuma, M. Takano, and Y. Bando, *J. Solid State Chem.* **95**, 230 (1991).
⁸ E. M. McCarron, M. A. Subramanian, J. C. Calabrese, and R. L. Harlow, *Mat. Res. Bull.* **23**, 1355 (1988).
⁹ P. W. Anderson, *Phys. Rev.* **79**, 350 (1950).
¹⁰ C. de Graaf, I. de P. R. Moreira, F. Illas, and R. L. Martin, *Phys. Rev. B* **60**, 3457 (1999).
¹¹ R. S. Eccleston, M. Uehara, J. Akimitsu, H. Eisaki, N. Motoyama, and S. I. Uchida, *Phys. Rev. Lett.* **81**, 1702 (1998).
¹² N. Ogita, Y. Fujita, Y. Sakaguchi, Y. Fujino, T. Nagata, J. Akimitsu, and M. Udagawa, *J. Phys. Soc. Jpn.* **69**, 2684 (2000).
¹³ S. M. Kazakov, S. Pachot, E. M. K. S. N. Putelin, E. V. Antipov, C. Chaillout, J. Capponi, P. G. Radaelli, and M. Marezio, *Physica C* **276**, 139 (1997).
¹⁴ M. Windt, M. Grüninger, T. Nunner, C. Knetter, K. P. Schmidt, G. S. Uhrig, T. Kopp, A. Freimuth, U. Ammerahl, B. Büchner, et al., *Phys. Rev. Lett.* **87**, 127002 (2001).
¹⁵ S. Brehmer, H.-J. Mikeska, M. Müller, N. Nagaosa, and S. Uchida, *Phys. Rev. B* **60**, 329 (1999).
¹⁶ M. Matsuda, K. Katsumata, R. S. Eccleston, S. Brehmer, and H.-J. Mikeska, *Phys. Rev. B* **62**, 8903 (2000).
¹⁷ T. S. Nunner, P. Brune, T. Kopp, M. Windt, and M. Grüninger, *Phys. Rev. B* **66**, 180404(R) (2002).
¹⁸ K. P. Schmidt, C. Knetter, M. Grüninger, and G. S. Uhrig, *Phys. Rev. Lett.* **90**, 167201 (2003).
¹⁹ A. Löffert, C. Gross, and W. Assmus, *J. Cryst. Growth* **237-239 (P1)**, 796 (2002).
²⁰ S. Sugai, T. Shinoda, N. Kobayashi, Z. Hiroi, and M. Takano, *Phys. Rev. B* **60**, R6969 (1999).
²¹ D. L. Rousseau, R. P. Bauman, and S. P. S. Porto, *J. Raman Spectrosc.* **10**, 253 (1981).
²² D. C. Johnston, M. Troyer, S. Miyahara, D. Lidsky, K. Ueda, M. Azuma, Z. Hiroi, M. Takano, M. Isobe, Y. Ueda, M. A. Korotin, V. I. Anisimov, A. V. Mahajan, and L. L. Miller, arXiv:cond-mat/0001147 (unpublished).
²³ Z. V. Popović, M. J. Konstantinović, V. A. Ivanov, O. P. Khuong, R. Gajić, A. Vietkin, and V. V. Moshchalkov, *Phys. Rev. B* **62**, 4963 (2000).
²⁴ A. Gozar, G. Blumberg, B. S. Dennis, B. S. Shastry, N. Motoyama, H. Eisaki, and S. Uchida, *Phys. Rev. Lett.* **87**, 197202 (2001).
²⁵ S. Sugai, and M. Suzuki, *Phys. Stat. Sol. B* **215**, 653 (1999).
²⁶ Note that the crystallographic directions of the rungs and legs are different in other ladder compounds.
²⁷ M. V. Abrashev, C. Thomsen, and M. Surtchev, *Physica C* **280**, 297 (1997).
²⁸ P. A. Fleury, and R. Loudon, *Phys. Rev.* **166**, 514 (1968).
²⁹ E. Müller-Hartmann, and A. Reischl, *Eur. Phys. J. B* **28**, 173 (2002).
³⁰ T. Kawada, and S. Sugai, *J. Phys. Soc. Jpn.* **67**, 3897 (1998).
³¹ W. A. Harrison, *Elementary electronic structure* (World Scientific Publishing Co. Pte. Ltd., 1999).
³² P. Knoll, C. Thomsen, M. Cardona, and P. Murugaraj, *Phys. Rev. B* **42**, 4842 (1990).
³³ K. Ishida, Y. Kitaoka, K. Asayama, M. Azuma, Z. Hiroi, and M. Takano, *J. Phys. Soc. Jpn.* **63**, 3222 (1994).
³⁴ K. Ishida, Y. Kitaoka, Y. Tokunaga, S. Matsumoto, K. Asayama, M. Azuma, Z. Hiroi, and M. Takano, *Phys. Rev. B* **53**, 2827 (1996).